RSC Advances

ROYAL SOCIETY OF CHEMISTRY

www.rsc.org/advances

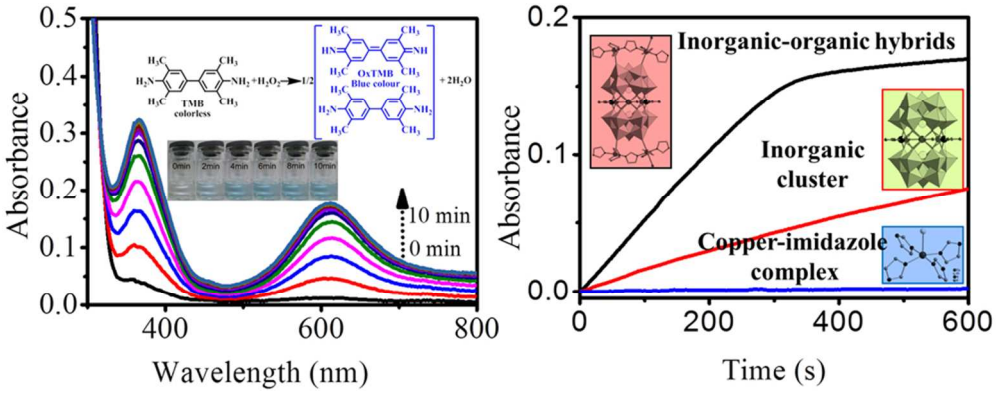

85x32mm (300 x 300 DPI)

ROYAL SOCIETY OF CHEMISTRY

ARTICLE

Synergistic Effect of Sandwich Polyoxometalates and Copper-Imidazole Complexes for Enhancing Peroxidase-like Activity†

Received 00th January 20xx,
Accepted 00th January 20xx

DOI: 10.1039/x0xx00000x

www.rsc.org/

Dong-Feng Chai,‡[b] Zhuo Ma,‡[d] Hong Yan,[b] YunFeng Qiu,*[a,e] Hong Liu,*[b] Hua-Dong Guo,[c] and Guang-Gang Gao*[b,c]

Two inorganic-organic hybrids based on copper(II)-imidazole complex modified sandwich-type tungstobismuthate or tungstoantimonite, $Na_4H_2[Cu_4(H_4im)_{12}(H_3im)_2][Cu_3(H_2O)_3(XW_9O_{33})_2]\cdot nH_2O$ (H_4im = imidazole, H_3im = deprotonated imidazole, X = Bi (**1**), *n* = 28 or X = Sb (**2**), *n* = 25) have been synthesized and structurally characterized by single crystal X-ray diffraction and FTIR. The sandwich polyoxoanion $[Cu_3(H_2O)_3(XW_9O_{33})_2]^{12-}$ is modified by two copper(II)-imidazole complexes to form **1** or **2**, in which an anionic imidazole is rarely observed as a linker to coordinate to two neighboring copper ions. As compared to other Keggin-type polyoxometalate based peroxidase-like mimics, **1** and **2** both demonstrate higher peroxidase-like activity using 3,3',5,5'-tetramethylbenzidine (TMB) as a peroxidase substrate in the presence of H_2O_2 around physiological pH values in heterogeneous phase. The maximized synergistic effects of sandwich-type POMs and copper(II)-imidazole complexes are responsible for the enhancement of peroxidase-like activity. The negatively charged POMs and non-covalent interactions between imidazole ligands and TMB are beneficial to increase the affinity of TMB substrate, and thus lead to higher sensitivity towards H_2O_2. Considering the dependence of TMB colour on H_2O_2 concentrations, compound **1** can be used as an effective probe to detect H_2O_2 through facile colorimetric method in a linear range from 1 μM to 50 μM with a low detection limit of 0.12 μM.

Introduction

H_2O_2 detection has attracted much attention in recent years due to its production may affect many biochemistry reactions in the body that is dangerous for human health.[1-3] This motivates us to develop various methods for detecting H_2O_2 amount in fundamental research or industrial field, even in live organism.[4] The commonly used optical H_2O_2 detection strategy involves a horseradish peroxidase (HRP) catalyzing a chromogenic substrate such as 3,3',5,5'-tetramethylbenzidine (TMB) to form the colored product.[5] Although this assay is effective, the inherent drawbacks of the natural enzyme, such as sensitivity of catalytic activity to environmental conditions, low operational stability, as well as time-consuming and expensive preparation and purification process, which restrict their practical applications.[6, 7] As a result, considerable efforts have been dedicated to the design and construction of novel enzyme mimics with similar functions as natural enzymes.[4, 8, 9] In recent years, since Fe_3O_4 magnetic nanoparticles were found to exhibit intrinsic peroxidase mimics activity,[2, 3] lots of nanomaterials including noble metal materials,[10, 11] metal oxides,[12] hybrid materials,[10] carbon-materials,[10, 13-15] polymers,[16] and nanocomposites[17, 18] have been developed and exhibited peroxidase-like mimics activities. However, most reported nanomaterials based artificial enzymes suffer from drawbacks including sophisticated preparation procedures, expensive preparation equipments, toxic reagents used in the synthesis, expensive starting materials, or relatively unsatisfied peroxidase-like performance.

Recently, organic-inorganic hybrids have attracted a lot of attention because of the combination of specific property of individual component and corresponding synergistic effect.[19-21] POMs are well-known metal-oxo-cluster compounds, which are emerging as potentially useful materials for numerous applications, such as nanocomposites, nanoelectronics and artificial enzymes in biology.[22, 23] However, only few enzyme mimics based on polyoxometalates (POMs) have been found to present enzyme mimics activity for the detection of H_2O_2, such as $[PW_{12}O_{40}]^{3-}$ and $[SiW_{12}O_{40}]^{4-}$ polyoxoanions.[24, 25] However, most of the reported POMs-based peroxidase-like studies are homogeneous, and suffer from recovery and environmental contamination. The coassembly of polyoxometalate with folate has been confirmed to possess

[a] State Key Laboratory of Urban Water Resource and Environment, Harbin Institute of Technology, Harbin 150090, China. E-mail: qiuyf@hit.edu.cn (Y. Qiu)
[b] Department of Chemistry, College of Pharmacy, Jiamusi University, Jiamusi 154004, China. E-mail: hliu@jmsu.edu.cn (H. Liu), gaogg@jmsu.edu.cn (G. Gao)
[c] Department of Chemistry, Changchun Normal University, Changchun 130032, China.
[d] School of Life Science and Technology, Harbin Institute of Technology, 92 West Dazhi Street, Harbin, Heilongjiang, 150001, P.R. China.
[e] Key Laboratory of Microsystems and Micronanostructures Manufacturing (Ministry of Education), Harbin Institute of Technology, Harbin 150080, China.

† Electronic Supplementary Information (ESI) available: [FTIR spectra of compounds and precursors, peroxidase-like activity on catalyst concentrations, steady-state kinetic assays of compound **2** and precursors, CV curves of compound **1** in the presence of H_2O_2, FTIR of compound **1** before and after reaction, SEM and EDX of compound **2** before and after reaction, selected bond lengths (Å) and angles (°) tables for compounds **1** and **2**]. See DOI: 10.1039/b000000x/

‡ These authors contributed equally to this work.

peroxidase-like activity and targeting ability towards folate acceptor over-expressed cells.[26, 27] However, the unsatisfied solubility of folate will hinder its coassembly with other types POMs based hybrid materials. Furthermore, these explored POMs are mainly classified as Keggin-type POMs or their derivatives, which can only maintain intact structure around acidic conditions, thus their applications are somehow limited.[28-30] Considering most biochemical reactions occurred at physiological pH conditions, the study of POMs possessing stability in physiological pH conditions should be emphasized, and more attention should be paid on the application as enzyme mimics for the detection of H_2O_2.[31, 32] In view of diverse POMs,[33] sandwich-type POMs are usually synthesized in weak acidic solutions, which may show synergistic effect with combined transitional metal ions and intriguing redox properties.[34-40] Wang et al. recently reported tetranuclear zirconium-substituted polyoxometalates with peroxidase-like activity, which indicates that the active catalytic species are ascribed to the unique structural feature of sandwiched {Zr_4} clusters but not the lacunary polyoxometalate anions themselves or the independent Zr ions.[41] However, the reaction time of TMB oxidation in Wang's work was 90 min, which still did not fulfill the stringent requirement of bio-detectors, which requires fast response.

Considering all the above mentioned issues, more efforts should be devoted to the design of hybrid composites based on sandwich-type POMs and exploration of their enzyme mimics activity. In contrast to common $[PW_9O_{34}]^{9-}$ or $[SiW_9O_{34}]^{9-}$ induced sandwich-type POMs, we pay much attention to sandwich complexes composed of $[BiW_9O_{33}]^{9-}$ or $[SbW_9O_{33}]^{9-}$ due to that these complexes usually include additional organic-transition-metal coordination subunits.[42-44] In addition, Cu_2O, CuO, or CuS was found to possess intrinsic enzyme mimics properties, whereas the true mechanism for the oxidation of TMB in the presence of H_2O_2 needed more deep insights. It is worth mentioning that the generated active •OH radicals were temporarily responsible for the whole process. Thus, three aspects are considered in present study: 1) The integration of sandwich-type POMs containing Cu subunits and Cu-imidazole complexes might generate synergistic effects on their redox properties around physiological pH level.[45] 2) The negatively charged nature of complexes including copper ions sandwiched by two $[BiW_9O_{33}]^{9-}$ units might contribute to the overall performance due to the enhanced affinity towards TMB (amine groups).[46] 3) The introduction of organic ligands may also enhance the affinity of hybrid materials to TMB due to the non-covalent interactions, such as hydrogen bonding or π-π stacking interactions, and thus increase their peroxidase-like activity for sensitive detection of H_2O_2.

Herein, two inorganic-organic hybrids based on imidazole-copper(II) complex modified sandwich-type tungstobismuthate or tungstoantimonite have been synthesized by conventional solution method, expressed as $Na_4H_2[Cu_4(H_4im)_{12}(H_3im)_2]$-$[Cu_3(H_2O)_3(XW_9O_{33})_2]\cdot nH_2O$ (H_4im = imidazole, H_3im = deprotonated imidazole, X = Bi (**1**), n = 28 or X = Sb (**2**), n = 25). The peroxidase-like activity of **1** or **2** was systematically investigated.

Experimental sections

Materials and methods

All reagents were purchased and used without further purification. Elemental analyses (C, H, and N) were performed on a Perkin-Elmer 2400 CHN Elemental Analyzer. Bi, Sb, W, Cu and Na were determined by a Leeman inductively coupled plasma (ICP) spectrometer. FTIR characterization was carried out on a BRUKER Vertex 70 FTIR spectrometer-with a KBr pellet in the 4000-400 cm^{-1} region. Scanning electron microscopy (SEM) and Energy dispersive X-ray (EDX) spectroscopy observations were performed on an FEI Quanta 200 scanning electron microscope. The acceleration voltage was set to 10 kV. The sample was stuck on the observation platform and sprayed with platinum vapor under high vacuum for about 90 s. All the reactions were monitored in time scan mode at 612 nm using a Hitachi UV2010 spectrophotometer. The apparent kinetic parameters were calculated based on the function $\nu = V_{max} \times [S]/(K_m + [S])$, where ν is the initial velocity, V_{max} is the maximal reaction velocity, [S] is the concentration of substrate and K_m is the Michaelis constant.[3]

X-ray Crystallography

Crystal data of **1** and **2** were collected on a Bruker SMART CCD APEX II diffractometer with a graphite monochromated Mo Kα (λ = 0.71073 Å) at 293 K. Selected data collection parameters and other crystallographic results are summarized in Table 1. All data were corrected for Lorentz polarization and absorption effects. The programs of SHELXS97 and SHELXL2014 were used for structure solution and refinement.[47, 48] Since some disordered solvent molecules and sodium ions could not be adequately modeled, they have been treated as a diffuse contribution to the overall scattering without specific atom positions by PLATON/SQUEEZE.[49] H atoms (N–H and C–H) were placed at calculated positions and were allowed to ride on the carrier-C/N atoms with U_{iso} = 1.2U_{eq}. The O atoms from water molecules are located from difference Fourier maps, but the H atoms of water molecules could not be located from difference Fourier maps and thus were not included in the final refinement. For **1** or **2**, parts of the identified water oxygen atoms were refined isotropically. The unidentified Na and water oxygen atoms around the polyoxoanion structure can not be resolved by structural analysis and thus were determined by thermogravimetric and elemental analyses. CCDC 676664 (**1**) and 676665 (**2**) contain the supplementary crystallographic data. These data can be obtained free of charge via www.ccdc.cam.ac.uk/data_request/cif.

Synthesis of compound 1 $Bi(NO_3)_3\cdot 5H_2O$ (0.241 g, 0.5 mmol) dissolved in 1 mL of 6 mol/L HCl was added to a solution of $Na_2WO_4\cdot 2H_2O$ (3.300 g, 10.0 mmol) in 30 mL of deionized water with stirring for about 20 min. Then, $Cu(Ac)_2\cdot H_2O$ (0.299 g, 1.5 mmol) and 1 mL aqueous solution of imidazole (0.074 g, 1.1 mmol) were added to the above solution successively, and the pH value was adjusted to 8.2 by addition of 1 mol/L NaOH. The mixture was kept at 80 °C for about 2 h and then cooled to

Table 1 Crystal data and structure refinement for compounds **1** and **2**.

	1	**2**
Empirical formula	$C_{42}H_{118}Bi_2Cu_7N_{28}Na_4O_{97}W_{18}$	$C_{42}H_{112}Sb_2Cu_7N_{28}Na_4O_{94}W_{18}$
Formula weight	6831.38	6602.89
Temperature	293 (2) K	293 (2) K
Wavelength	0.71073 Å	0.71073 Å
Crystal system	Monoclinic	Monoclinic
space group	*P*21/m	*P*21/m
a (Å)	14.052 (2)	14.0510 (13)
b (Å)	32.528 (3)	32.530 (3)
c (Å)	17.992 (2)	17.9902 (17)
α (°)	90	90
β (°)	103.462 (2)	103.461(10)
γ (°)	90	90
Volume (Å^3)	7997.9 (16)	7997.0 (13)
Z, Calculated density	2, 2.836 Mg·m^{-3}	2, 2.742 Mg·m^{-3}
Absorption coefficient	16.075 mm^{-1}	14.219 mm^{-1}
F (000)	5820.2	5736.0
Limiting indices	$-17 \le h \le 17$, $-40 \le k \le 40$, $-22 \le l \le 22$	$-17 \le h \le 17$, $-40 \le k \le 39$, $-21 \le l \le 22$
Measured reflections	67709	69047
Independent reflections	15934	16113
Data/restraints/parameters	15934/1/744	16113/1/812
$R_{(int)}$	0.1479	0.1053
Goodness-of-fit on F^2	0.990	0.998
R_1,[a] wR_2[b] [$I > 2\sigma(I)$]	0.0577, 0.0888	0.0478, 0.0754
R_1,[a] wR_2[b] (all data)	0.1305, 0.0990	0.0963, 0.0827

[a] $R_1 = \Sigma \, || F_o| - | F_c|| / \Sigma \, | F_o|$. [b] $wR_2 = | \Sigma w (|F_o|^2 - |F_c|^2)| / \Sigma | w (F_o^2)^2|^{½}$.

room temperature and filtrated. Slow evaporation at room temperature resulted in gray blue crystals (0.557 g, yield 37.0% based on Cu) of **1** after 7 days. Anal. calcd for $C_{42}H_{118}Bi_2Cu_7N_{28}Na_4O_{97}W_{18}$: Cu, 6.51; Bi, 6.12; W, 48.44; Na, 1.35%; C, 7.38; N, 5.74; H, 1.74%. Found: Cu, 6.42; Bi, 6.04; W, 47.98; Na 1.36; C, 7.49; N, 5.82; H, 1.77%. IR (KBr disk): 3480(s), 3300(s), 3030(w), 2951(w), 2879(w), 2830(w), 1627(s), 1537(m), 1502(w), 1417(w), 1328(m), 1261(m), 1174(w), 1130(w), 1072(s), 935(s), 887(s), 717(s), 513(w), 445(m) cm^{-1} (Fig. S1A).

Synthesis of compound 2 Compound **2** was synthesized by the similar procedure with **1** except that the $Bi(NO_3)_3{\cdot}5H_2O$ was replaced by $SbCl_3$ (0.114 g, 0.5 mmol). Purple-blue crystals of **2** (0.448 g, yield 30.2% based on Cu) formed after 7 days. Anal. Calcd for $C_{42}H_{112}Sb_2Cu_7N_{28}Na_4O_{94}W_{18}$: Cu, 6.74; Sb, 3.69; W, 50.12; Na, 1.39; C, 7.64; N, 5.94; H, 1.71%. Found: Cu, 6.69; Sb, 3.67; W, 49.89; Na, 1.40; C, 7.73; N, 6.01; H, 1.74%. IR (KBr disk): 3470(s), 3200(w), 3060(w), 2946(w), 2869(w), 2830(w), 1625(s), 1540(m), 1502(w), 1417(w), 1326(m), 1260(m), 1172(w), 1124(w), 1072(s), 939(s), 887(s), 726(s), 513(w), 442(m) cm^{-1} (Fig. S1B).

Peroxidase-like activity of 1 or 2 To investigate the peroxidase-like activity of **1** or **2**, the catalytic oxidation of the peroxidase substrate TMB in the presence of H_2O_2 was measured. In a typical colorimetric experiment, unless otherwise stated, the reaction solution consists of 50 μM of TMB, 100 μM of H_2O_2, and 1.38×10^{-2} mg/mL of compound **1** in pH = 5.5 acetate buffer solution at 55 °C. Afterwards the sample in cuvette was positioned immediately in the cell holder of UV-vis spectrophotometer for the steady-state kinetic measurements which were implemented in time course mode by monitoring the absorbance changes at 612 nm. The steady-state kinetics of compound **1** (1.38×10^{-2} mg/mL) were performed by varying one of the concentrations of H_2O_2 (60, 80 and 100 μM) and fixing the other of the concentrations of TMB (50 μM), or varying one of the concentrations of TMB (50, 75 and 100 μM) and fixing the other of the concentrations of H_2O_2 (100 μM). Other steady-state kinetics are similar except the catalysts concentrations were replaced, for example, compound **2** (1.34×10^{-2} mg/mL), BiW_9Cu_3 (1.13×10^{-2} mg/mL) and SbW_9Cu_3 (1.10×10^{-2} mg/mL). All the reaction was monitored by measuring the absorbance at 612 nm of TMB in 0.1 M, pH = 5.5 acetate buffer solution at 55 °C.

Results and discussion

Synthesis and structure analysis

1 and **2** were synthesized by treating a suspension of $Na_2WO_4{\cdot}2H_2O$, $Bi(NO_3)_3{\cdot}5H_2O$ (or $SbCl_3$), $Cu(Ac)_2{\cdot}H_2O$, and N-donor ligand imidazole at 80 °C. The successful syntheses indicate that the copper(II)-imidazole is an effective subunit in such reaction system to modify the sandwich-type POMs. Both the molar ratio of $Na_2WO_4{\cdot}2H_2O$ to $Bi(NO_3)_3{\cdot}5H_2O$ (or $SbCl_3$) and the pH value are the key factors for synthesizing these two complexes. Only the molar ratio of 20:1 for $Na_2WO_4{\cdot}2H_2O$ to

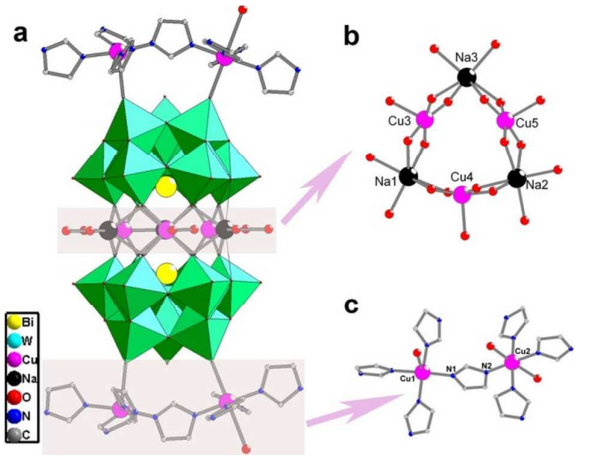

Fig. 1 Structure of compound (a) **1**, (b) Cu_3Na_3 cluster between two BiW_9 subunits, and (c) $Cu_2(H_4im)_6(H_3im)$ complex in polar positions. All the isolated Na^+, water and H atoms are omitted for clarity.

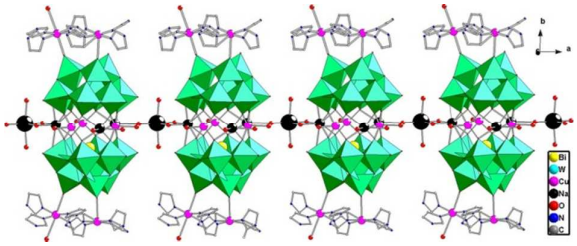

Fig. 2 1D structure of compound **1**.

$Bi(NO_3)_3{\cdot}5H_2O$ (or $SbCl_3$) can successfully produce complexes **1** and **2**. The pH value should be strictly controlled from 8.16 and 8.25 for **1** and **2**, respectively. Under our optimal synthetic conditions, the synthesis of compound **1** and **2** are highly reproducible. Single crystal X-ray diffraction analyses reveal that compounds **1** and **2** are isomorphous POM-Cu-imidazole complexes, of which the unit cell dimensions, volumes, related bond distances and angles are only slightly changed. Thus, we discuss the structure of **1** in detail as a typical example.

In compound **1**, the trivacant α-B-$[XW_9O_{33}]^{9-}$ unit in the two compounds derives from the parent-Keggin structure by taking off three edge-sharing WO_6 octahedra. The presence of a lone electron pair prevents the formation of the closed Keggin type structure. Each α-B-$[XW_9O_{33}]^{9-}$ unit provides six oxygen donor atoms coming from six W atoms to coordinate with the central metal cluster. The central hetero atom Bi(III) or Sb(III) is surrounded pyramidally by three oxygen atoms. For the Cu ions in the central belt, each copper ion in a square-pyramidal geometry is coordinated by four terminal oxygen atoms from four WO_6 groups of two different $[BiW_9O_{33}]^{9-}$ units with Cu–O bond lengths of 1.940(13)-1.962(12) Å and an oxygen atom from water with Cu–O bond lengths of 2.28(2)-2.31(2) Å. In addition to the three Cu(II) ions, polyoxoanion **1** also incorporates three Na ions within the central belt (Fig. 1). Each sodium ion is coordinated by four oxygen atoms from two $[BiW_9O_{33}]^{9-}$ units and two terminal water molecules to furnish

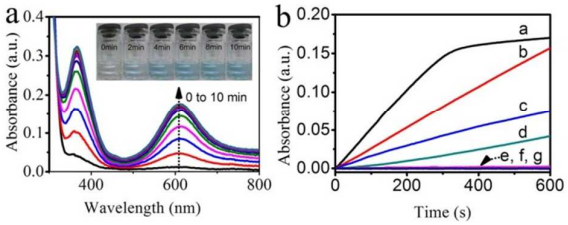

Fig. 3 (a) UV-vis absorption spectra of compound **1** catalyzed TMB colorimetric system as a function of reaction time from 0 to 10 min. Inset in (a): photographs of corresponding reaction solutions with increasing reaction time. (b) Typical time-dependent absorbance changes of TMB solutions catalyzed by different systems. Curves from a to g represent (a) **1** (1.38×10^{-2} mg/mL), (b) **2** (1.34×10^{-2} mg/mL), (c) BiW_9Cu_3 (1.13×10^{-2} mg/mL), (d) SbW_9Cu_3 (1.10×10^{-2} mg/mL), (e) $Cu(im)_4Cl_2$ (0.55×10^{-2} mg/mL), (f) **1** (1.38×10^{-2} mg/mL) without H_2O_2 and (g) **1** (1.38×10^{-2} mg/mL) without TMB in acetate buffer solution (pH = 5.5), H_2O_2 100 μM and TMB 50 μM at 55 °C recorded for 600 s.

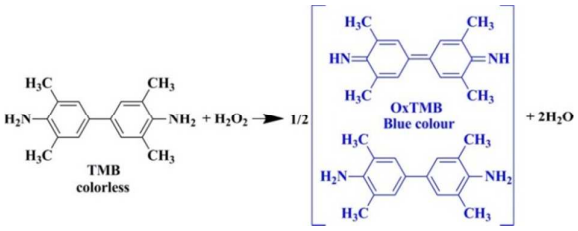

Scheme 1 The oxidation reaction of TMB by compound **1** or **2** in the presence of H_2O_2.

a $\{NaO_6\}$ octahedral geometry. Three such Na ions together with three Cu ions alternately lie in the central belt between two $[BiW_9O_{33}]^{9-}$ anions. Interestingly, in polar positions, two usual Cu-imidazole complexes further coordinate to terminal oxygen atoms from WO_6 groups with Cu–O bond lengths of 2.391(13)-2.493(13) Å. In Cu-imidazole subunit, each Cu coordinates to four imidazole ligands with Cu–N bond lengths of 1.932(17)-2.025(17) Å. Most interestingly, one of the imidazole ligand simultaneously coordinates to two Cu ions, of which the anionic coordination mode of imidazole is firstly shown among the known Cu(II)-imidazole complexes. In addition, by the linkage of Na^+ ions, compound **1** forms a 1D chain structure along *a* axis, as shown in Fig. 2.

Peroxidase-like activity evaluation

The catalytic peroxidase-like activities of both compounds are evaluated under different reaction conditions. First, compound **1** was added into TMB solution in the absence of H_2O_2. Even large amount of H_2O_2 (1 mM) was used in reaction, the solution maintained colourless, indicative of the insufficient activity of H_2O_2 towards the oxidation of TMB, which is consistent with most previous work.[15, 24, 25] In contrast, inset in Fig. 3a shows the photographs of TMB solutions with increasing reaction time in the presence of **1** and H_2O_2. It is clear to see the blue colour in 10 min, which is a typical phenomenon resulting from the oxidized TMB. The oxidized TMB structure is displayed in the scheme 1. It is worthwhile mentioning that only 2 min was required to observe colour change by naked eyes for **1**, but a longer time of 90 min was needed for previous reported sandwich-type POMs based enzyme mimics.[41] Furthermore, the process was recorded by

monitoring the TMB absorbance change at 612 nm in Fig. 3a. An obvious absorbance peak at 612 nm appears for the TMB/H_2O_2/**1** system, consistent with previous result.[41] The characteristic peak position is slightly different with that of HRP (652 nm), which might be due to the non-covalent interactions between POMs units and TMB. Similarly, compound **2** can also catalyze the oxidation of TMB by H_2O_2 to produce the typical blue colour, but showing less catalytic activity than that of compound **1**. Meanwhile, control experiments in Fig. 3b showed that the blue colour of TMB/H_2O_2/**1** or TMB/H_2O_2/**2** was much deeper than all the control groups, such as $Na_{12}[Cu_3Bi_2W_{18}O_{66}]\cdot 32H_2O$ (BiW_9Cu_3), $Na_{12}[Cu_3Sb_2W_{18}O_{66}]\cdot 32H_2O$ (SbW_9Cu_3), and $Cu(im)_4Cl_2$.[50, 51] Further, the solutions of TMB/**1** and H_2O_2/**1** maintain colourless under similar reaction conditions. These results indicate that compounds **1** and **2** indeed possessed peroxidase-like activity which can be tentatively explained as follows. On the one hand, the negatively charged sandwich-type POMs not only act as catalytic sites, but also enhanced the absorption of TMB due to electrostatic interactions. On the other hand, imidazole ligands will further contribute to enhance the affinity of hybrid materials to TMB due to hydrogen bonding or π-π stacking interactions. These synergistic effects results in highly improved catalytic performance than pristine POMs without organic ligands, which has been verified in control experiments. The higher peroxidase-like activity of **1** than **2** might be ascribed to the hetero-atoms possessing different redox properties, which would affect the intrinsic peroxidase-like activity. In the following text, compound **1** was used as a representative model to evaluate the peroxidase-like activity.

Similar to HRP and other enzyme mimics,[3, 4, 8] the catalytic activities of compound **1** are also dependent on catalyst amounts, pH, and temperature, respectively. The reaction can reach equilibrium in 10 min when 1.38×10^{-2} mg/mL catalyst was applied (Fig. S2). The reaction pH-dependent response curves were shown in Fig. 4a. When the pH value increased from 5.0 to 5.5, the absorbance increased slightly. After exceeding this point, the absorbance decreased gradually as increasing pH values. Therefore, pH 5.5 was selected as the optimal pH values. Comparing with Keggin POMs based enzyme mimics, the optimal pH value for our compounds was higher, which might be ascribed to the synthetic conditions of our crystals. As stated in synthetic section, the pH values were strictly controlled from 8.16 to 8.25 for compound **1** and **2**. Taking inspiration from previous work on the synthesis of sandwich-type POMs, pH values below 7 will lead to the decomposition of crystalline structures, and further cause the transformation to other kinds of chemical structures, such as Keggin structure.[52] It is also worthwhile mentioning that the peroxidase-like activity of $H_3PW_{12}O_{40}$ can be only obtained at pH 3.0, and almost lost all the activity above this pH value. However, as shown in Fig. 4a, above 80% relative activity was maintained in the pH values ranging from 5.0 to 7.0. Thus, our hybrid crystals might expand their application as enzyme

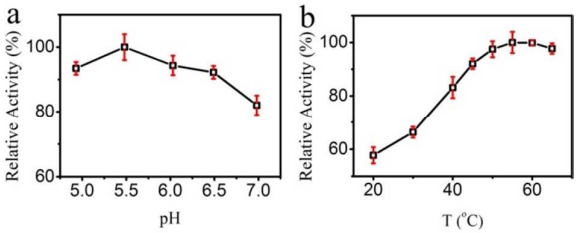

Fig. 4 Dependence of the peroxidase-like activity on the (a) pH (4.5, 5, 5.5,6, 6.5) and (b) T (20, 30, 40, 45, 50, 55, 60, 65 °C) of compound **1** (1.38×10^{-2} mg/mL), 100 μM H_2O_2 and 50 μM TMB.

mimics around physiological pH conditions.[53] Meanwhile, in Fig. 4b the reaction temperature-dependent response curves were also examined. The absorbance at 612 nm increased gradually with the increasing temperature, and reaches the maximum at 55 °C. Under our experimental conditions, the optimal catalyst amount, pH and temperature for compound **1** are 1.38×10^{-2} mg/mL, 5.5, and 55 °C, respectively.

Inspired from biomolecular enzymes, Michaelis-Menten model is widely accepted to evaluate the behavior of enzyme mimics. For POMs based peroxidase-like mimics, the surface atoms acting as real active species might possess non-covalent interactions towards TMB or H_2O_2, and synergistic effect among all components will also contribute to catalytic performance. The Michaelis-Menten curve was plotted according to Lineweaver-Burk plotting method by the following equation: $\frac{1}{v} = \frac{K_m}{V_{max}} \cdot \frac{1}{[S]} + \frac{1}{V_{max}}$. First, to investigate the mechanism of the peroxidase-like activity of compound **1**, the apparent steady-state kinetic parameters were evaluated in Fig. 5a and 5b by changing the concentrations of TMB or H_2O_2, respectively. In this experiment, the kinetic data were obtained by varying one substrate concentration and fixing the other. TMB containing two amine groups is selected as a typical chromogenic substrate, yielding a strong affinity toward the negatively charged POMs. The apparent steady-state kinetic parameters for the reactions catalyzed by compound **2** and two POMs precursors are displayed in Fig. S3, S4 and S5, respectively. As demonstrated by the calculated catalytic parameters in Table 2, the apparent K_m value for compound **1** with TMB as substrate was smaller than that of HRP, suggesting that compound **1** had higher affinity for TMB than HRP. The K_m value of compound **1** was slightly lower than corresponding POMs clusters when using TMB as substrate, proving that compound **1** had a higher affinity for TMB than POMs clusters. Meanwhile, the apparent K_m value for compound **1** with H_2O_2 as substrate was lower than that of HRP, also indicating that compound **1** had higher affinity for H_2O_2 than HRP. In addition, the K_m values for compound **1** were lower than those of corresponding POMs cluster using TMB or H_2O_2 as substrates, confirming that compound **1** had higher affinity for TMB than POMs cluster. We have also performed cyclic voltammetry (CV) experiment of compound **1** as representative in Fig. S6. Obvious signals of electro-catalytic reduction of H_2O_2 on glass carbon electrode (GC) modified with compound **1** were observed, which might be related to the electro-catalytic reduction ability of compound **1** and high affinity between H_2O_2 and compound **1**. The above results are consistent with our assumption that the introduction of

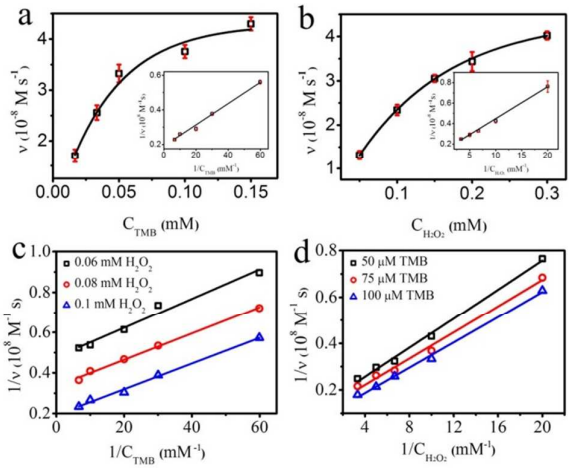

Fig. 5 Steady-state kinetic assays of compound **1**. (a) H_2O_2 concentration was kept constant at 100 μM and TMB concentration was varied. (b) TMB concentration was maintained at 50 μM and H_2O_2 concentration was varied. (c and d) Double reciprocal plots of the activity of compound **1** with the concentration of one substrate (H_2O_2 or TMB) fixed. The reaction was performed in compound **1** (1.38×10^{-2} mg/mL) and 0.1 M, pH = 5.5 acetate buffer solution at 55 °C.

Table 2. Comparson of Michaelis-Menten parameters for our hybrids and other enzyme mimics.

Enzyme mimics	K_m (mM)		V_{max} (10^{-8} M S^{-1})		Ref.
	TMB	H_2O_2	TMB	H_2O_2	
PW_{12}	0.11	15.89	43.1	4.24×10^{-4}	24
Fe_2SiW_{10}	—	0.014	—	14.24	26
PMV	0.41×10^{-3}	—	470	—	27
Fe_3O_4	0.098	154	3.44	9.78	3
HRP	0.434	3.7	10.00	8.71	3
BiW_9Cu_3	0.36	0.29	1.43	0.69	This work
SbW_9Cu_3	0.14	0.25	0.64	0.71	This work
1	0.03	0.23	5.25	7.33	This work
2	1.24	2.32	3.02	3.44	This work

organic ligands will facilitate the absorption of TMB or H_2O_2, which are two important factors for the enhancement of catalytic performance.

To further study the catalytic mechanism of hybrid compounds, the peroxidase-like activity over a range of TMB and H_2O_2 concentrations were performed. As shown in Fig. 5c and 5d, the double reciprocal plots of initial velocity versus the concentration of one substrate were obtained over a range of concentrations of the second substrate. It is obvious that the slopes of all lines were almost parallel, indicating the possible ping-pong mechanism.[3] Namely, hybrid compounds bind and react with the first substrate and then release the first product before reacting with the second substrate.

It has been reported that the nature of TMB catalytic reaction may originate from the generation of hydroxyl radical (•OH) from the decomposition of H_2O_2. The sequences of reaction responsible for the blue colour of TMB might contain two steps. In the first step, H_2O_2 adsorbed over hybrid compound **1** and then activated by the synergistic effects of BiW_9Cu_3 and

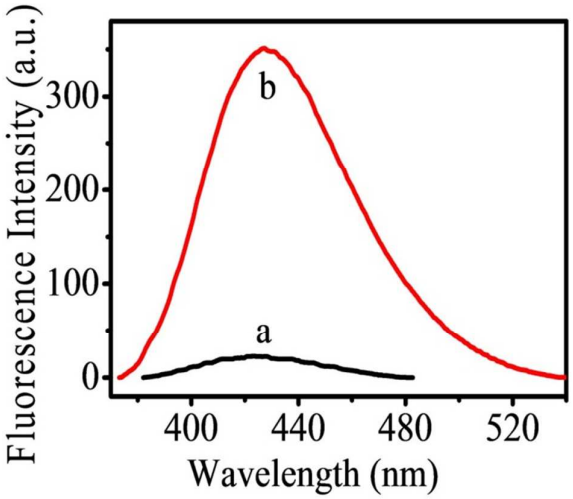

Fig. 6 Fluorescence spectra of TA solution (2×10^{-3} M) in the presence of H_2O_2 (200 mM) and different amount of compound **1**. (a) 0 mg and (b) 2 mg during photoluminescence probing technique, respectively.

$Cu_2(H_4im)_6(H_3im)$ complex. The generated •OH then quantitatively oxidize TMB to blue colour. Terephthalic acid (TA) photoluminescence probing techniques was used to confirm the formation of •OH, which is widely applied in detection of hydroxyl radical due to high sensitivity and selectivity.[54] TA was non-fluorescent in the absence of compound **1**, whereas, the non-luminescent TA is converted to highly fluorescent 2-hydroxy terephthalic acid (HTA) in the presence of compound **1**. During this process, HTA is a product of TA reacted with •OH. As displayed in Fig. 6, the fluorescence intensity of the solution containing compound **1** was 15 times higher than that in the absence of compound **1**. This result illustrates that our hybrid compounds could activate H_2O_2 to generate •OH radical.

The reproducibility of peroxidase-like mimics plays an important role for practical application. It is well known that natural enzyme activity severely deteriorates after exposure to high temperature. For example, the enzyme activity of HRP dramatically declined after treatment at elevated temperature above 40 °C for only 2h. In contrast, the enzyme activity of compound **1** was stable when it was incubated at a wide range of temperatures from 20 to 65 °C for 12h. pH value in solution is of great importance for maintaining the integrity of POMs structures. In our study, pH value of 5.5 was optimal to evaluate the peroxidase-like activity of hybrid compounds for its highest activity. The stability of compound **1** was further examined by SEM, EDX (Fig. 7) and FTIR (Fig. S7) spectra before and after reaction, compound **2** was further examined by SEM and EDX (Fig. S8) spectra. Some structural defects on the surface of crystals in Fig. 7A and 7B might be resulted from the etching effect of solvents or stirring damage.[55] EDX spectroscopy of **1** before and after reaction in Fig. 7C and 7D confirmed the relative ratio of Bi, W, and Cu are almost maintained, confirming the basic crystal structure is intact during reaction. According to our hypothesis, the intact structure will guarantee the synergistic effect for maximizing

the peroxidase-like activity of our hybrid compounds. And this assumption is also supported by the steady-state kinetic assays experiments, compound **1** exhibits better activity than individual POMs cluster or copper and imidazole complex. As shown in Fig. S7, the absorption bands of BiW_9Cu_3 cluster

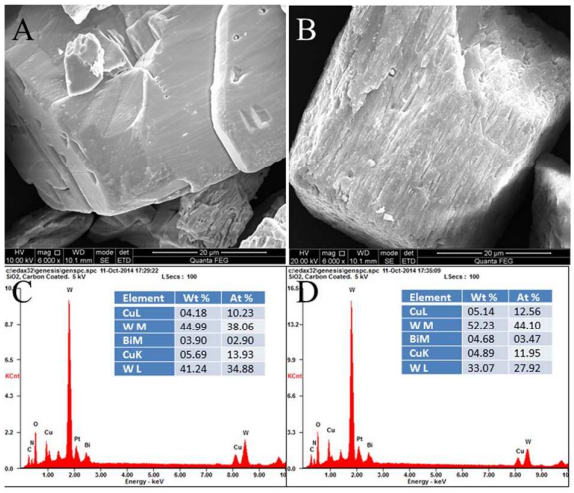

Fig. 7 (A) and (B) SEM images of ground compound **1** before and after reaction; (C) and (D) Corresponding EDX before and after reaction. EDX are measured for three times to check out the consistency.

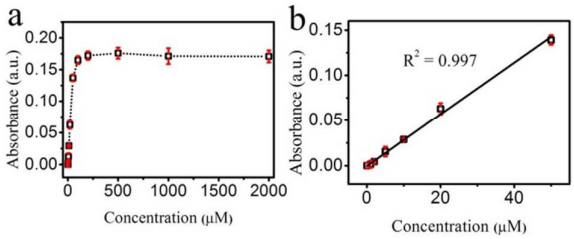

Fig. 8 H_2O_2 in 3 mL acetate buffer solution (0.1 M, pH = 5.5) including compound **1** (1.38 × 10^{-2} mg/mL) at 55 °C. (a) Dose–response curves for the detection of H_2O_2 concentration from 1 μM to 2000 μM. (b) Linear fitting of dose–response curves for H_2O_2 from 1 μM to 50 μM.

located at 941, 891 and 719 cm^{-1} are corresponding to the W-O_d, W-O_b, and W-O_c stretching vibrations. These three main characteristic peaks of as-synthesized crystals arising from W-O_d, W-O_b, and W-O_c stretching vibrations are maintained, which are centered at 935, 887 and 717 cm^{-1}, indicating the slight variations in electron distribution and structural distortion of POMs due to the strong coordination interaction between POMs and $Cu_2(H_4im)_6(H_3im)$ complex.[56] Furthermore, these three main characteristic peaks of crystals after catalytic reaction are maintained, which appeared at 939, 885 and 738 cm^{-1}. The slight position differences are ascribed to the structural distortion of POMs after reaction. Comparing with previous reported enzyme mimics based on Keggin-type POMs, the optimal activity was realized at higher pH values of 5.5 than PW_{12} of 3.0, which is highly related to the optimal synthetic conditions of sandwiched POMs.[52] The robustness of hybrid compounds at higher temperature and pH value makes them as promising materials in bio-applications.[57, 58]

Finally, we investigate the potential application of compound **1** as peroxidase-like mimics to detect H_2O_2. Since the colour of TMB solution is dependent on the concentration of H_2O_2 in the presence of compound **1**, colorimetric detection of H_2O_2 can be realized easily using our method. Fig. 8 shows typical H_2O_2 concentration-response curves. There is a plateau after adding 50 μM H_2O_2. The linear range for H_2O_2 was from 1 to 50 μM with limit of detection (LOD) of 0.12 μM ($\mathrm{LOD} = \mathrm{K}\ S_0/S$, where K is a numerical factor selected according to the confidence level desired, S_0 is the standard deviation (S.D.) of the blank measurements (n = 10, K = 3) and S is the slope of calibration curve.)[59] This detection method based on our hybrid compounds system gave a lower LOD than the method using Fe_3O_4 system.[3]

Conclusions

In this work, we present two inorganic-organic hybrids based on sandwich-type tungsto-bismuthate/antimonite anions and copper(II) complex moieties, of which an interesting anionic imidazole is firstly demonstrated among the known Cu(II)-imidazole complexes. Further exploration indicates that compounds **1** and **2** both present enhanced peroxidase-like activity for the detection of H_2O_2 around physiological pH than common Keggin-type $[PW_{12}O_{40}]^{3-}$ polyoxoanion. The enhanced peroxidase activity of our compounds was ascribed to the synergistic effects of sandwich-type POMs and copper(II)-imidazole complexes. The negatively charged POMs and non-covalent interactions between ligands and TMB were responsible for the high affinity of TMB substrate, and thus result in the higher sensitively detecting ability toward H_2O_2. Our work will facilitate the utilization of sandwich-type POMs based hybrid compounds as sensitive peroxidase mimics for medical diagnostics and biotechnology.

Acknowledgements

This work is supported by the Open Project of State Key Laboratory of Urban Water Resource and Environment, Harbin Institute of Technology (No. ES201514), National Natural Science Foundation of China (No. 21271034), Heilongjiang Universities' Science and Technology Innovation Team program (2012TD010), Heilongjiang Province Department of Education Science and Technology Research Project (12541792), China Postdoctoral Science Foundation Funded Project (No. 20100471047, 2012T50335).

Notes and references

1 H. Jin, D. A. Heller, M. Kalbacova, J.-H. Kim, J. Zhang, A. A. Boghossian, N. Maheshri and M. S. Strano, *Nat. Nanotechnol.*, 2010, **5**, 302-309.
2 H. Wei and E. Wang, *Anal. Chem.*, 2008, **80**, 2250-2254.
3 L. Gao, J. Zhuang, L. Nie, J. Zhang, Y. Zhang, N. Gu, T. Wang, J. Feng, D. Yang, S. Perrett and X. Yan, *Nat. Nanotechnol.*, 2007, **2**, 577-583.

4 V. Carroll, B. W. Michel, J. Blecha, H. VanBrocklin, K. Keshari, D. Wilson and C. J. Chang, *J. Am. Chem. Soc.*, 2014, **136**, 14742-14745.
5 F. Olucha, F. Martínez-García and C. López-García, *J. Neurosci. Meth.*, 1985, **13**, 131-138.
6 C. Mateo, J. M. Palomo, G. Fernandez-Lorente, J. M. Guisan and R. Fernandez-Lafuente, *Enzyme Microb. Technol.*, 2007, **40**, 1451-1463.
7 N. C. Veitch, *Phytochemistry*, 2004, **65**, 249-259.
8 H. Wei and E. Wang, *Chem. Soc. Rev.*, 2013, **42**, 6060-6093.
9 Y. Lin, J. Ren and X. Qu, *Acc. Chem. Res.*, 2014, **47**, 1097-1105.
10 J.-W. Zhang, H.-T. Zhang, Z.-Y. Du, X. Wang, S.-H. Yu and H.-L. Jiang, *Chem. Commun.*, 2014, **50**, 1092-1094.
11 X. Jiang, C. Sun, Y. Guo, G. Nie and L. Xu, *Biosens. Bioelectron.*, 2015, **64**, 165-170.
12 L. Zhang, L. Han, P. Hu, L. Wang and S. Dong, *Chem. Commun.*, 2013, **49**, 10480-10482.
13 J. Zhang, Y. Liu, Y. Li, H. Zhao and X. Wan, *Angew. Chem., Int. Ed.*, 2012, **51**, 4598-4602.
14 Y. Song, K. Qu, C. Zhao, J. Ren and X. Qu, *Adv. Mater.*, 2010, **22**, 2206-2210.
15 Z. Wang, X. Lv and J. Weng, *Carbon*, 2013, **62**, 51-60.
16 Y. Tao, E. Ju, J. Ren and X. Qu, *Chem. Commun.*, 2014, **50**, 3030-3032.
17 A. Asati, S. Santra, C. Kaittanis, S. Nath and J. M. Perez, *Angew. Chem., Int. Ed.*, 2009, **48**, 2308-2312.
18 Y.-L. Dong, H.-G. Zhang, Z. U. Rahman, L. Su, X.-J. Chen, J. Hu and X.-G. Chen, *Nanoscale*, 2012, **4**, 3969-3976.
19 Z. Guo, X. Song, H. Lei, H. Wang, S. Su, H. Xu, G. Qian, H. Zhang and B. Chen, *Chem. Commun.*, 2015, **51**, 376-379.
20 X. Zhao, X. Bu, Q.-G. Zhai, H. Tran and P. Feng, *J. Am. Chem. Soc.*, 2015, **137**, 1396-1399.
21 Y. Yang, J. Yang, P. Du, Y.-Y. Liu and J.-F. Ma, *CrystEngComm*, 2014, **16**, 1136-1148.
22 G.-J. Cao, J.-D. Liu, T.-T. Zhuang, X.-H. Cai and S.-T. Zheng, *Chem. Commun.*, 2015, **51**, 2048-2051.
23 P. Gouzerh and A. Proust, *Chem. Rev.*, 1998, **98**, 77-112.
24 J.-J. Wang, D.-X. Han, X.-H. Wang, B. Qi and M.-S. Zhao, *Biosens. Bioelectron.*, 2012, **36**, 18-21.
25 S. Liu, J.-Q. Tian, L. Wang, Y.-W. Zhang, Y.-L. Luo, H.-Y. Li, A. M. Asiri, A. O. Al-Youbi and X.-P. Sun, *ChemPlusChem*, 2012, **77**, 541-544.
26 C. Sun, X. Chen, J. Xu, M. Wei, J. Wang, X. Mi, X. Wang, Y. Wu and Y. Liu, *J. Mater. Chem. A*, 2013, **1**, 4699-4705.
27 J. Wang, X. Mi, H. Guan, X. Wang and Y. Wu, *Chem. Commun.*, 2011, **47**, 2940-2942.
28 C. Rocchiccioli-Deltcheff, M. Fournier, R. Franck and R. Thouvenot, *Inorg. Chem.*, 1983, **22**, 207-216.
29 X. López, J. M. Maestre, C. Bo and J.-M. Poblet, *J. Am. Chem. Soc.*, 2001, **123**, 9571-9576.
30 W.-C. Chen, L.-K. Yan, C.-X. Wu, X.-L. Wang, K.-Z. Shao, Z.-M. Su and E.-B. Wang, *Cryst. Growth Des.*, 2014, **14**, 5099-5110.
31 O. Blokhina, E. Virolainen and K. V. Fagerstedt, *Ann. Bot.*, 2003, **91**, 179-194.
32 S.-X. Chen and P. Schopfer, *Eur. J. Biochem.*, 1999, **260**, 726-735.
33 H. Lv, W. Guo, K. Wu, Z. Chen, J. Bacsa, D. G. Musaev, Y. V. Geletii, S. M. Lauinger, T. Lian and C. L. Hill, *J. Am. Chem. Soc.*, 2014, **136**, 14015-14018.
34 N. Gao, H. Sun, K. Dong, J. Ren, T. Duan, C. Xu and X. Qu, *Nat. Commun.*, 2014, **5**, 10.1038/ncomms4422.
35 A. Rubinstein, P. Jiménez-Lozanao, J. J. Carbó, J. M. Poblet and R. Neumann, *J. Am. Chem. Soc.*, 2014, **136**, 10941-10948.
36 U. Kortz, N. K. Al-Kassem, M. G. Savelieff, N. A. Al Kadi and M. Sadakane, *Inorg. Chem.*, 2001, **40**, 4742-4749.
37 R. Al-Oweini, B. S. Bassil, J. Friedl, V. Kottisch, M. Ibrahim, M. Asano, B. Keita, G. Novitchi, Y. Lan, A. Powell, U. Stimming and U. Kortz, *Inorg. Chem.*, 2014, **53**, 5663-5673.
38 L. Huang, S.-S. Wang, J.-W. Zhao, L. Cheng and G.-Y. Yang, *J. Am. Chem. Soc.*, 2014, **136**, 7637-7642.
39 H.-Y. Zhao, J.-W. Zhao, B.-F. Yang, H. He and G.-Y. Yang, *Cryst. Growth Des.*, 2013, **13**, 5169-5174.
40 X.-B. Han, Z.-M. Zhang, T. Zhang, Y.-G. Li, W. Lin, W. You, Z.-M. Su and E.-B. Wang, *J. Am. Chem. Soc.*, 2014, **136**, 5359-5366.
41 D. Li, H. Han, Y. Wang, X. Wang, Y. Li and E. Wang, *Eur. J. Inorg. Chem.*, 2013, **2013**, 1926-1934.
42 H. N. Miras, L. Vila-Nadal and L. Cronin, *Chem. Soc. Rev.*, 2014, **43**, 5679-5699.
43 D.-Y. Du, J.-S. Qin, S.-L. Li, Z.-M. Su and Y.-Q. Lan, *Chem. Soc. Rev.*, 2014, **43**, 4615-4632.
44 H. Liu, C. Qin, Y.-G. Wei, L. Xu, G.-G. Gao, F.-Y. Li and X.-S. Qu, *Inorg. Chem.*, 2008, **47**, 4166-4172.
45 W. Chen, J. Chen, Y.-B. Feng, L. Hong, Q.-Y. Chen, L.-F. Wu, X.-H. Lin and X.-H. Xia, *Analyst*, 2012, **137**, 1706-1712.
46 Y. Jv, B. Li and R. Cao, *Chem. Commun.*, 2010, **46**, 8017-8019.
47 G. M. Sheldrick, *Acta Cryst*. 2008, **A64**, 112-122.
48 G. M. Sheldrick, *Acta Cryst*. 2015, **C71**, 3-8.
49 A. L. Spek, *Acta Cryst*. 2009, **D65**, 148-155.
50 C. Rosu, D. Rasu and T. R. Weakley, *J. Chem. Crystallogr.*, 2003, **33**, 751-755.
51 B.-D. Wu, Z.-N. Zhou, Y.-G. Bi, L. Yang, J.-G. Zhang and T.-L. Zhang, *Z. Anorg. Allg. Chem.*, 2013, **639**, 799-803.
52 E. B. Wang, C. W. Hu and L. Xu, *Concise of Polyoxometalate Chemistry, Chemical Industry Press, Beijing*, 1998.
53 J. T. Rhule, C. L. Hill, D. A. Judd and R. F. Schinazi, *Chem. Rev.*, 1998, **98**, 327-358.
54 A.-L. Hu, Y.-H. Liu, H.-H. Deng, G.-L. Hong, A.-L. Liu, X.-H. Lin, X.-H. Xia and W. Chen, *Biosens. Bioelectron.*, 2014, **61**, 374-378.
55 C. Mondal, J. Pal, K. K. Pal, A. K. Sasmal, M. Ganguly, A. Roy, P. K. Manna and T. Pal, *Cryst. Growth Des.*, 2014, **14**, 5034-5041.
56 Y.-Q. Lan, S.-L. Li, X.-L. Wang, K.-Z. Shao, D.-Y. Du, H.-Y. Zang and Z.-M. Su, *Inorg. Chem.*, 2008, **47**, 8179-8187.
57 M. Yang, D. Xu, L. Jiang, L. Zhang, D. Dustin, R. Lund, L. Liu and H. Dong, *Chem. Commun.*, 2014, **50**, 4827-4830.
58 N. Dube, J. W. Seo, H. Dong, J. Y. Shu, R. Lund, L. M. Mahakian, K. W. Ferrara and T. Xu, *Biomacromolecules*, 2014, **15**, 2963-2970.
59 J. Chen, H. Chen, C. Zhou, J. Xu, F. Yuan and L. Wang, *Anal. Chim. Acta*, 2012, **713**, 111-114.